

Crystal structures of the Tie2 receptor ectodomain and the angiopoietin-2–Tie2 complex

William A Barton^{1,2}, Dorothea Tzvetkova-Robev², Edward P Miranda¹, Momchil V Kolev¹, Kanagalaghatta R Rajashankar¹, Juha P Himanen¹ & Dimitar B Nikolov¹

The Tie receptor tyrosine kinases and their angiopoietin (Ang) ligands play central roles in developmental and tumor-induced angiogenesis. Here we present the crystal structures of the Tie2 ligand-binding region alone and in complex with Ang2. In contrast to prediction, Tie2 contains not two but three immunoglobulin (Ig) domains, which fold together with the three epidermal growth factor domains into a compact, arrowhead-shaped structure. Ang2 binds at the tip of the arrowhead utilizing a lock-and-key mode of ligand recognition—unique for a receptor kinase—where two complementary surfaces interact with each other with no domain rearrangements and little conformational change in either molecule. Ang2–Tie2 recognition is similar to antibody–protein antigen recognition, including the location of the ligand-binding site within the Ig fold. Analysis of the structures and structure-based mutagenesis provide insight into the mechanism of receptor activation and support the hypothesis that all angiopoietins interact with Tie2 in a structurally similar manner.

The development of the adult cardiovascular system involves the differentiation of endothelial cells from precursor angioblasts and their subsequent migration, growth and sprouting^{1–3}. This arises as a result of two distinct processes termed vasculogenesis (formation of major primitive blood vessels) and angiogenesis (remodeling and extension of the adult vasculature)^{3,4}. Although vasculogenesis occurs during only the initial stages of development, angiogenesis is continually required in the adult for normal wound repair. Angiogenesis also occurs during solid tumor growth and development, resulting in an enriched nutrient and oxygen supply^{3–7}. The angiopoietins and Tie proteins are central in both developmental and tumor-induced angiogenesis. Tie2 overexpression has been documented in breast, ovarian and hepatocellular tumors, as well as in glioblastomas^{8–11}, reaching the highest levels in the peripheral neovascular endothelium of invasive tumors^{8,11}. Administration of soluble Tie2 ectodomain reduces vascular length density and tumor growth *in vivo*^{12,13}, presumably by depleting available ligand.

Tie receptors, comprised of Tie1 and Tie2, are type 1 transmembrane protein RTKs¹⁴. Tie2 interacts with all four angiopoietins^{15–17}, whereas no ligands have yet been identified for the closely related Tie1. The ectodomains of the two receptors each contain three Ig domains, three epidermal growth factor (EGF) repeats and three fibronectin type III repeats (Fig. 1a). Domain-deletion analysis indicates that the Ig–EGF region of Tie2 mediates angiopoietin recognition and binding^{18,19}.

The four known angiopoietins each contain an N terminus that modulates angiopoietin clustering (superclustering region), followed

by a rather large coiled-coil motif and a fibrinogen-like region at the C terminus^{14–17} (see below). Binding experiments have documented that the fibrinogen region mediates the interactions with Tie2 (ref. 19,20). The coiled-coil and the superclustering motifs are also required for signaling because they mediate ligand oligomerization, which is necessary for receptor activation^{18,20,21}. Indeed, all angiopoietins exist primarily as tetramers, hexamers and higher-order oligomers in solution^{16,18,20,22}. To gain a more accurate molecular understanding of the angiopoietin–Tie2 interactions, we determined the structures of the human Tie2 ectodomain and the Ang2–Tie2 complex.

RESULTS

Overall structure of the Tie2 ectodomain

The crystal structure of the Tie2 ectodomain (see Methods), illustrated in Figure 1, reveals an arrowhead-shaped molecule with approximate dimensions of 90 × 65 × 50 Å. It contains three Ig (Ig1–Ig3) and three EGF (EGF1–EGF3) domains, which are compactly folded onto one another, with an extensive amount of surface area buried by inter-domain intramolecular interactions. The surface loops of Ig2 are at the tip of the Tie2 arrowhead, whereas Ig3 lies at its base. One of the arrowhead sides is formed by Ig1 and the other by the EGF region, specifically by EGF3. At the core of the structure are EGF1 and EGF2, which pack against the outer four domains (the three Igs and EGF3) and hold them together. Clear electron density for at least one *N*-acetylglucosamine moiety was observed in all four potential glycosylation sites, corresponding to Asn140 and Asn158 in Ig2 as well as

¹Structural Biology Program, Memorial Sloan-Kettering Cancer Center, 1275 York Avenue, New York, New York 10021, USA. Present addresses: Department of Biochemistry, Virginia Commonwealth University, Richmond, Virginia 23298, USA (W.A.B.) and NE-CAT, Advanced Photon Source, Argonne, Illinois 60439, USA (K.R.R.). ²These authors contributed equally to this work. Correspondence should be addressed to D.B.N. (nikolovd@mskcc.org).

Received 21 March; accepted 2 May; published online 28 May 2006; doi:10.1038/nsmb1101

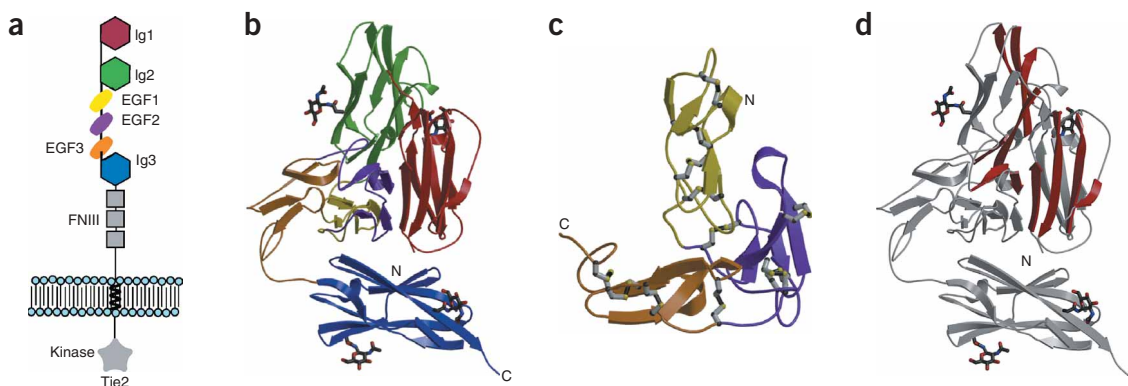


Figure 1 Structure of the Tie2 ligand-binding region. **(a)** Schematic representation of the domain organization of the Tie receptors. Red, Ig1; blue, Ig2; green, Ig3; yellow, EGF1; purple, EGF2; orange, EGF3; gray, the three fibronectin type III (FNIII) repeats and the cytoplasmic tyrosine kinase catalytic domain. **(b)** The ligand-binding extracellular region of Tie2, colored as in **a**. Asparagine-linked carbohydrate groups are shown in ball-and-stick format. **(c)** The EGF region of Tie2, colored as in **a**. The 12 disulfide bonds (four in each EGF repeat) are shown in gray ball-and-stick format. **(d)** The Tie2 ligand-binding region. Red, the large and highly curved *trans*-domain 11-stranded β -sheet comprised of strands Ig1(D-E-B-A)-EGF2(C-D)-Ig2(A'-G-F-C-C').

Asn399 and Asn438 in Ig3 (**Fig. 1b**). Fourteen disulfide bonds stabilize the structures of the individual Tie2 domains: one each is present in Ig1 and Ig3, and four in each of the EGF repeats.

Tie2 Ig and EGF domains

Many cell-surface signaling receptors contain Ig domains as ligand-recognition modules²³, including most members of the RTK superfamily²⁴. Notably, the crystal structure of Tie2 reveals that the molecule contains not two, as previously suggested^{25,26}, but three immunoglobulin-like domains. Indeed, the N-terminal Tie2 domain (Ig1) was not previously recognized as such because it lacks appreciable sequence homology to other immunoglobulin domains, including even the structurally similar Tie2 Ig2 and Ig3.

Immunoglobulin domains are commonly classified into V, C1, C2 and I sets^{23,27}. The three Ig domains of Tie2 are variants of the I set, members of which consist of two β -sheets formed by strands ABED and A'GFCC' (**Fig. 2**). It should be noted, though, that the Tie2 domains are structurally not very closely related to other Ig domains, but are more similar to one other and superimpose with r.m.s. deviations between equivalent C α positions of 1.8–2.0 Å. Nevertheless, there are substantial deviations between Tie2 Ig1, Ig2 and Ig3. For example, analogous to the division of the C set into C1 and C2 subsets, a subdivision of the I set into I1 and I2 has been suggested, depending on whether or not a D strand is present²⁸. According to this classification, Ig1 and Ig3 are topologically closer to the I1 subset and Ig2 to the I2 subset.

Ig1 (Tie2 residues 23–120) contains two four-stranded β -sheets, ABED and A'GFC (**Fig. 2**), and a short α -helix. It deviates from the canonical I1 topology because it lacks the C' strand, a fact that has also been reported for other I-subset members, such as Axonin²⁹. A disulfide bond, buried in the hydrophobic core (Cys44-Cys102), bridges the two Ig1 β -sheets. Ig2 comprises residues 122–209, forming one three-stranded (ABE) and one five-stranded (A'GFCC') β -sheet. It also contains two short helices, but, unlike Ig1 and Ig2, no disulfide bonds. Ig2 is structurally most similar to the Fv fragment of an antibody to a carbohydrate³⁰ and the myelin oligodendrocyte glycoprotein³¹, with an r.m.s. deviation between 90 equivalent C α positions of \sim 2.7 Å. It should be noted that both of these Ig2 homologs have a V-set topology, which differs from the I-set in that it has an extra C'' strand. Of all Tie2 domains, Ig3 (residues 348–442) has the closest to a

canonical I-subset topology and structurally most resembles the I subset's founding member, telokin²⁷.

In addition to the three Ig domains, Tie2 contains three EGF repeats with similar folding topologies, including two two-stranded β -sheets (AB and CD) and a short α -helix (**Figs. 1** and **2**). The α -helix is always positioned between strands C and D, forming a characteristic strand-helix-strand structural motif. In EGF1 and EGF2, the α -helix packs against the AB β -sheet of the same EGF repeat, whereas in EGF3, it points away, interacting instead with the EGF1 helix on one side and with Ig1 and Ig2 on the other. The three EGF domains form an L-shaped structure (**Fig. 1c**) that is distinct from other structurally characterized EGF repeat-containing proteins.

Tie2 interdomain interactions

The Tie2 ectodomain has a unique architecture in that the Ig and EGF domains fold intimately together into a compact globular structure. Specifically, Ig1 folds back onto the rest of the molecule and forms extensive hydrophobic and van der Waals interactions with Ig2, Ig3, EGF1 and EGF2. A flexible loop between EGF3 and Ig3 permits the latter to interact with the N terminus of Ig1 and to participate in extensive contacts with the underside of EGF1. At the center of the structure, EGF2 bridges Ig1 and Ig2. Specifically, the CD β -sheet of EGF2 inserts between strand A of Ig1 and strand A' of Ig2, creating a continuous, expansive, 11-stranded antiparallel β -sheet (red in **Fig. 1d**) spanning the entire core of the Tie2 ectodomain fold.

The surface area buried upon packing of the individual Tie2 domains into the final structure is unusually large, at approximately 3,800 Å². Indeed, nearly 20% of all Tie2 residues (80 of 430; see **Fig. 2**) participate in interdomain interactions. Many of the contacts involve polar residues engaged in hydrogen bonds and salt bridges. Notably, though, half of the buried residues (40 of 80) are hydrophobic, mediating van der Waals interactions. These would be surface exposed if the Tie2 ectodomain adopted an extended conformation, which would be energetically highly unfavorable. The three Ig and three EGF domains, therefore, can only be stable upon formation of the compact and rigid three-dimensional architecture illustrated in **Figure 1b**. Consequently, domain-deletion mutagenesis is not effective in identification of the precise ligand-interacting receptor regions¹⁸.

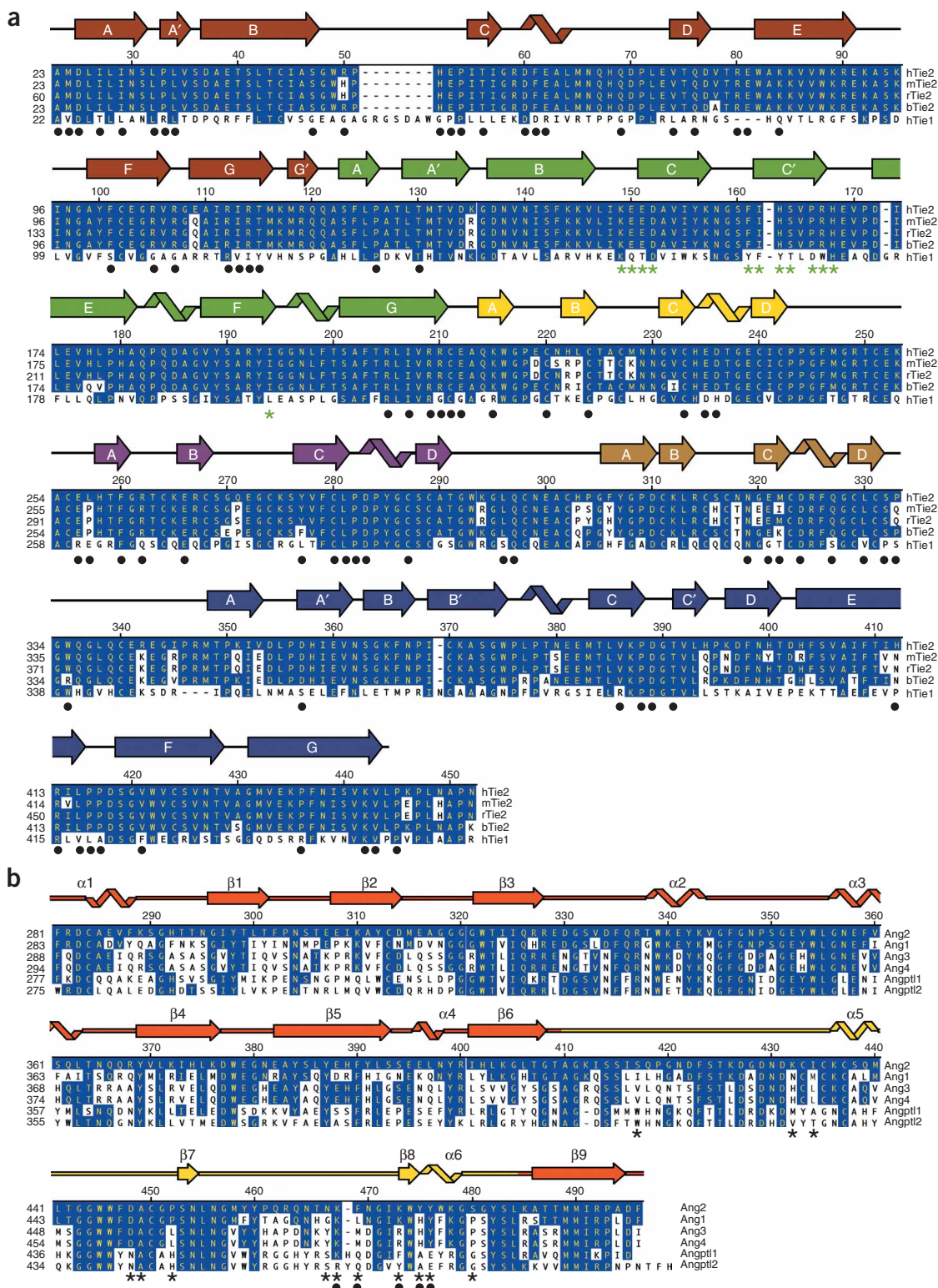


Figure 2 Sequence alignment of the interacting domains of angiopoietins and Ties. **(a)** Structure-based sequence alignment of human (h), mouse (m), rat (r) and bovine (b) Tie2 and human Tie1. Secondary structural elements are shown above alignment and colored as in **Figure 1**. β -strands are labeled according to the immunoglobulin fold convention²⁷. Black dots below alignment mark residues involved in interdomain intramolecular interactions; green asterisks mark residues involved in interactions with Ang2 in the structure of the Ang2-Tie2 complex. **(b)** Structure-based sequence alignment of the fibrinogen-like regions of the four angiopoietins and two angiopoietin-like proteins (Angpt11 and Angpt12). Regions of sequence identity to Ang2 are indicated. Secondary structure elements are noted above the sequences and colored as in **Figure 1**. Black asterisks mark residues involved in interactions with Tie2 in the structure of the Ang2-Tie2 complex; black dots mark residues identified by mutagenesis¹⁹ as important for Tie2 binding.

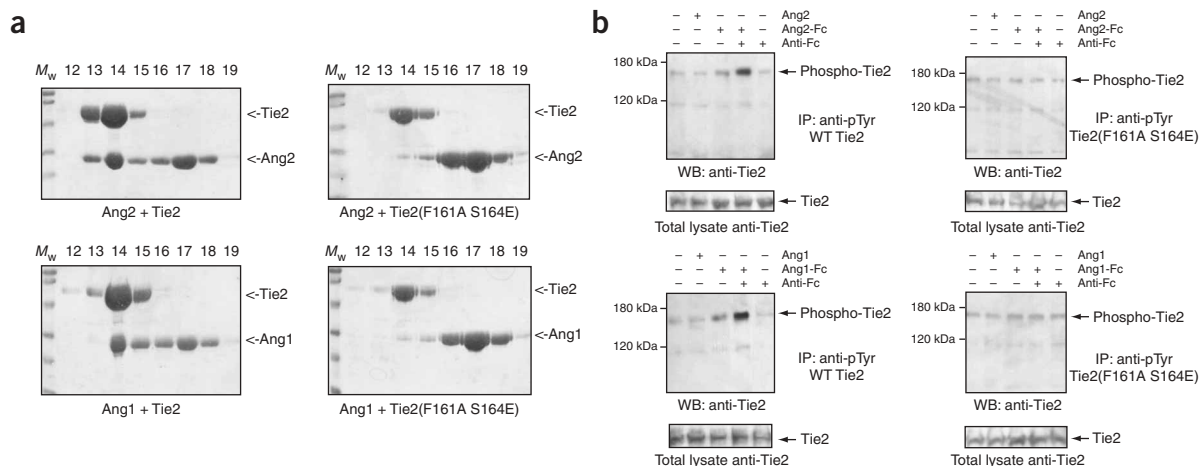


Figure 3 Ligand binding and activation of wild-type and mutant Tie2. **(a)** Migration of wild-type and mutant Tie2 mixed with either Ang1 or Ang2 (angiopoietins are in 2:1 molar excess) on gel-filtration columns. The fractions (in ml) are indicated above the lanes and the protein positions on the SDS-PAGE are indicated on the right. Leftmost lanes contain molecular weight markers. Left gels, Tie2 forms stable complexes with both Ang1 and Ang2, which elute with an apparent molecular weight of ~ 70 kDa. The unbound (excess) angiopoietins elute with an apparent molecular weight of ~ 20 kDa. Right panels, Tie2 containing substitutions of crucial ligand-binding residues (F161A and S164E) does not form a stable complex with either Ang2 or Ang1. **(b)** Activation of wild-type and mutant Tie2 receptors in stably transfected HEK293 cells by Ang1 and Ang2. Cells were treated with monomeric (Ang1 or Ang2), dimeric (Ang1-Fc or Ang2-Fc) or multimeric (Ang1-Fc or Ang2-Fc with anti-Fc) ligands 30 min before lysis. Anti-phosphotyrosine (pTyr) immunoprecipitates from lysates were analyzed by western blotting with an anti-Tie2. The overall Tie2 expression levels (bottom gels) were evaluated by probing the total cell lysates with anti-Tie2. Left gels, multimeric, but not monomeric, Ang1 and Ang2 induce phosphorylation of the Tie2 RTK. Right gels, neither Ang1 nor Ang2 induces phosphorylation of the mutated (F161A S164E) Tie2 receptor.

Structure of the Ang2–Tie2 complex

Our gel-filtration experiments (Fig. 3 and ref. 19) suggest that the interacting regions of Ang2 and Tie2, in the absence of the Ang2 coiled-coil and superclustering motifs, bind each other with a 1:1 stoichiometry. Indeed, the crystal structure of their complex (Methods) reveals a heterodimeric ligand-receptor assembly. Ang2 binds at the tip of the arrowhead-shaped Tie2, interacting with only the Ig2 domain of Tie2. Consequently, the Ang2–Tie2 complex has an elongated shape, with overall dimensions of $130 \times 65 \times 50$ Å (Fig. 4). The C terminus of Tie2, which points toward the cellular membrane of the Tie2-expressing cell, and the N terminus of Ang2, which connects to the coiled-coil and superclustering ligand regions, are located on the opposite sides of the complex.

The overall structure of Tie2 in the complex is similar to that of the unbound receptor. Considering the numerous Tie2 interdomain interactions, it is noteworthy that ligand binding does not cause any rearrangements in the receptor. Indeed, there is no change in the packing of the individual Ig and EGF domains against each other, and the bound and free Tie2 can be superimposed with an r.m.s. deviation between equivalent C α positions of 0.72 Å. The only apparent conformational change involves Ig2 strand C', which is shifted by 1.0–2.6 Å toward the incoming Ang2 so that Ig2 can make multiple interactions with several of Ang2's surface loops. The largest displacement occurs around Ig2 residue His163, the C α of which is shifted by ~ 2.6 Å from its position in the unbound receptor, enabling this residue to make a van der Waals contact with Ang2.

The Ang2 receptor-binding region has a compact three-domain fibrinogen-like fold¹⁹. In keeping with the established nomenclature of the domain architecture¹⁹, which follows that of human fibrinogen^{32,33}, we refer to the three domains in the Ang2 receptor-binding region as A, B and P (containing a bound Ca²⁺). Ang2 undergoes little structural change upon Tie2 binding. Indeed, its receptor-bound and

free structures can be superimposed with an r.m.s. deviation between equivalent C α positions of 0.55 Å, a value comparable to the experimental error in coordinate positions of structures determined at this resolution. The conformational changes are minor even at the ligand-receptor interface: Ser480 undergoes the greatest displacement, one of about 1.8 Å toward the incoming receptor, so that its side chains form a hydrogen bond with a main chain hydroxyl in Tie2. The Ang2 Ca²⁺-binding loop also shifts by approximately 0.5–1.0 Å toward the receptor (discussed further below).

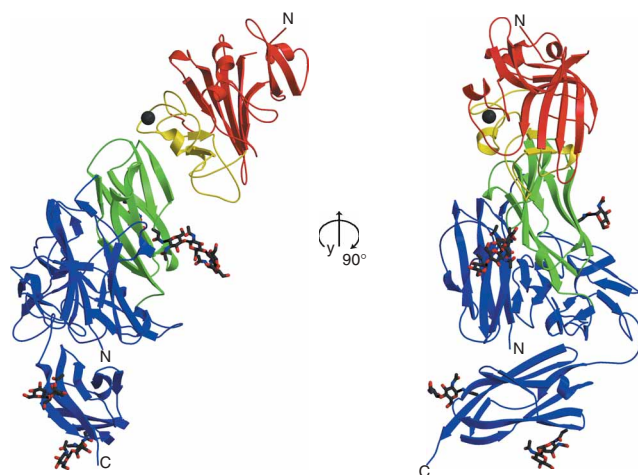
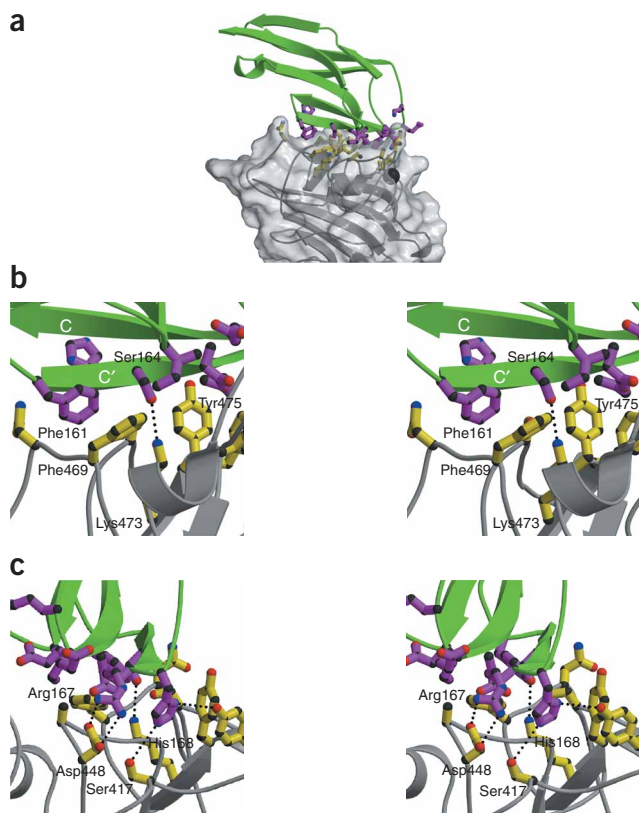


Figure 4 Crystal structure of the Ang2–Tie2 complex. Shown are two views of the complex related by a 90° rotation around the y-axis. Yellow, P domain of Ang2; red, the rest of Ang2; green, Tie2 Ig2; blue, the rest of Tie2; black sphere, bound Ca²⁺. Asparagine-linked carbohydrate groups are shown in ball-and-stick format.



Ligand-receptor interface

The ligand-receptor interface is confined to the top of the Tie2 Ig2 domain, which interacts with the P domain of Ang2 near the Ca²⁺-binding site (Figs. 4 and 5). Specifically, loops $\beta 6$ - $\alpha 5$, $\alpha 5$ - $\beta 7$, $\beta 7$ - $\beta 8$ and $\alpha 6$ - $\beta 9$, strand $\beta 8$ and helix $\alpha 6$ of Ang2 interact with the B-C, C-C' and F-G loops and strands C and C' of Tie2. The interface is continuous, burying approximately 1,300 Å² of molecular surface, and is dominated by van der Waals interactions between nonpolar side chains. At its center, hydrophobic residues from strand C' and the adjacent loops in Tie2 are engaged in contacts with residues from loops $\beta 7$ - $\beta 8$, $\alpha 5$ - $\beta 7$ and $\alpha 6$ - $\beta 9$ and helix $\alpha 6$ of Ang2. The aromatic ring of Tie2 Phe161 (Fig. 5b), for example, stacks against the aromatic ring of Ang2 Phe469 while also making a contact with the C β of Asn467. The adjacent Pro166 in Tie2 makes several contacts with Ang2 residues including Pro452, Tyr475 and Tyr476. Ang2 Pro452 also interacts with Tie2 His168. Finally, Ile194 in the Tie2 F-G loop contacts Ile434 and Phe469 from Ang2.

In addition to the hydrophobic interactions, an intricate hydrogen bond network, involving both side chain and main chain atoms, further stabilizes the Ang2-Tie2 complex. As previously mentioned, the side chain of Ang2 Ser480 makes a hydrogen bond with the main chain hydroxyl of Ser164 in Tie2. The side chain of the latter, by contrast, is within hydrogen-bonding distance of Ang2 Lys473. Asp152 of Tie2 deeply penetrates Ang2, making two hydrogen bonds with the main chain carboxyl group of Ala449 and the main chain amino group of Cys451. Notably, both nitrogens in the Tie2 His168 imidazole ring hydrogen bond, with the side chain hydroxyls of Ang2 Ser417 and Tyr476, respectively (Fig. 5c). Salt bridges are also present at the ligand-receptor interface. Specifically, Tie2 Arg167 binds Ang2 Asp448. In addition, Ang2 Lys432 is in a position to make a salt bridge with either Glu150 or Glu151 in Tie2,

but the electron density for its side chain is weak, making its precise position uncertain.

Role of the Ca²⁺ ion in receptor binding

The angiotensins contain a Ca²⁺-binding site that is structurally conserved among fibrinogen domain-containing proteins. Oxygen atoms of two side chains, as well as main chain carbonyl oxygens, chelate the Ca²⁺ ion. In Ang2, the side chains of the conserved Asp429 and Asp431 contribute one interacting oxygen each, and the carbonyl oxygen atoms of Cys433 and Cys435 complete the Ca²⁺-binding site. The Ca²⁺ ion is located close to the Ang2-Tie2 interface but is not directly involved in receptor binding (Figs. 4 and 5). Instead, it organizes and stabilizes the structure of the receptor-binding $\beta 6$ - $\alpha 5$ loop.

Angiotensin-2 recognition by Tie2

Most cell-surface receptors, and in particular the RTKs, contain relatively large, multidomain extracellular regions²⁴. Ligand binding often causes substantial rearrangements in the receptor ectodomains that are coupled to changes in their cell-surface oligomerization and are transduced to the inside of the cell, activating downstream signaling cascades²⁴. The structure of the Ang2-Tie2 complex, by contrast, reveals an unusual mode of RTK interaction with a ligand, where no major conformational changes or domain rearrangements are observed in its extracellular region. The recognition by Tie2 of its angiotensin ligand proceeds by a lock-and-key mechanism, where molecular surfaces that are complementary both in shape (shape complementarity value³⁴ of 0.61) and in chemical nature recognize and bind each other without marked rearrangements in either binding partner. In this respect, Tie2 seems to interact with its angiotensin ligands in a manner similar to the way antibodies bind antigens^{35,36}. In Tie2, as in most structurally characterized antibodies, the changes upon binding are confined mostly to side chain rearrangements, with the only main chain movements being shifts of contact residues toward the incoming ligand.

In a further analogy to antibody-antigen recognition, Tie2 binds Ang2 using cell-surface loops that are structurally equivalent to the hypervariable complementarity-determining regions (CDRs) that form the antigen-binding sites of antibodies. Figure 6a illustrates this similarity, comparing the structures of Tie2 Ig2 and its closest structural homolog, the Fv fragment of an antibody to a carbohydrate³⁰, and highlighting in yellow the positions of the Ang2-interacting loops of Tie2 and the anti-carbohydrate Fv CDRs. Furthermore, the surface area of a typical antibody-protein antigen contact is relatively small, in the 600–1,000 Å² range, similar in size to that of the Ang2-Tie2 area of contact. Finally, the Ang2-Tie2 interface has a very similar amino acid composition to most antibody-protein antigen interfaces, which are rich in aromatic residues, particularly tyrosines and tryptophans^{35,36}. In both cases, enthalpic forces drive the binding

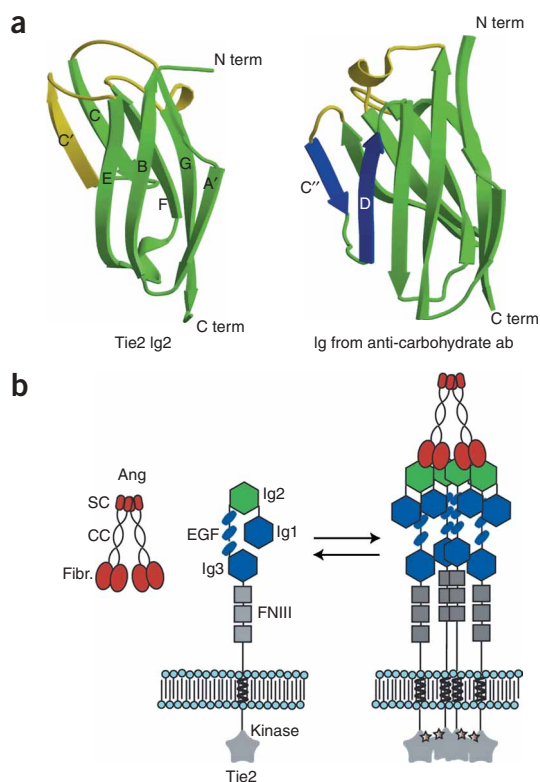


Figure 6 A model for Tie2 activation by angiopoietins. **(a)** Comparison of the structures of the ligand-binding Ig2 domain of Tie2 and its closest structural homolog, the antigen-binding Ig domain of an anti-carbohydrate (PDB entry 1MFA)³⁰. Note that Tie2 Ig2 lacks the D strand of a typical immunoglobulin I topology. The antibody Ig domain contains two extra β -strands (blue) that are not present in Tie2 Ig2: a D strand as well as a C' strand that is typical of an immunoglobulin V topology. Tie2 Ig2 secondary structure elements involved in ligand binding, as well as the hypervariable CDRs of the antibody, are in yellow. **(b)** Domain organization of the angiopoietins and Tie2 and a model for Tie2 activation. SC, superclustering region; CC, coiled-coil region; Fibr., fibrinogen-like region; FNIII, fibronectin type III repeats. Binding of the multimeric angiopoietins to Tie2 clusters the receptor, bringing into close proximity its kinase domains, which phosphorylate each other (stars) in *trans*, resulting in receptor activation and initiation of downstream signaling.

reaction, with the vast majority of the interacting residues being engaged in either hydrophobic van der Waals contacts or hydrogen bonds.

The fibrinogen P domain as a protein-interaction module

The structure of the Ang2–Tie2 complex reveals that the Ang2 P domain is solely responsible for mediating the interactions with Tie2 (Fig. 4). This is consistent with the results of previous structure-based mutagenesis of Ang2 (ref. 19), which correctly localized the interaction surface to a small region containing a cluster of residues conserved within the angiopoietin family but not among functionally distinct angiopoietin-like proteins that do not bind Tie2. Notably, the ligand-binding sites in the fibrinogen domains of tachylectin 5A (ref. 37) and human fibrinogen³³ are also located in this surface region of the P domain¹⁹, indicating that the fibrinogen domain has evolved as a flexible interaction module used by a variety of functionally unrelated proteins to interact with a variety of structurally unrelated binding partners. The angiopoietin receptor-binding regions contain two other surface patches of conserved residues located outside of the P domain¹⁹, but our structure, as well as previous structure-based mutagenesis¹⁹, document that they are not directly involved in receptor recognition. Instead, they could mediate, for example, interactions between the individual angiopoietin monomers in the multimeric assemblies formed by the full-length molecules.

Recognition of other angiopoietins by Tie2

The different angiopoietins exert different biological effects on Tie2-expressing cells. For example, in virtually all studied cases, the cellular response to Ang1 is consistent with Tie2-receptor activation, whereas Ang2 seems to be able to act in a context-dependent manner as either Tie2 agonist or antagonist^{17,18,20}. Ang3 and Ang4 are less well studied; it is believed that Ang3 is similar in function to Ang2, whereas Ang4 is

similar to Ang1 (ref. 15). The mechanistic basis of the different, even sometimes opposing, functions of Ang1 and Ang2 is unknown, but there could be several possible explanations. First, the receptor-binding domains of Ang2 and Ang1 could bind Tie2 in completely different manners, consecutively causing different rearrangements in the receptor. For example, Ang1 could bind in a way promoting an orientation of adjacent Tie2 molecules that facilitates activation of their kinase domains, whereas Ang2 binding could facilitate an inhibitory receptor orientation. Second, the Ang1–Tie2 and Ang2–Tie2 interfaces could be similar, but different oligomerization states of the ligands might cause different receptor responses. In this way, Ang1 and Ang2 could, for example, induce different downstream signaling pathways via different temporal activation patterns of Tie2. A similar behavior has been reported for members of the Eph receptor kinase family, where different biological responses have been attributed to different oligomerization states of the activating ligand³⁸. Third, Ang1 and Ang2 could interact with Tie2 in an identical fashion, but additional interactions of either the angiopoietins or Tie2 with other cell-specific receptors or coreceptors could induce different cellular responses.

The structure of the Ang2–Tie2 complex indicates that Ang1 would bind Tie2 in the same way as Ang2. Indeed, an examination of the ligand-receptor interface reveals that six of the thirteen contact residues are conserved between Ang2 and Ang1 (Fig. 2a). In addition, two residues contain conservative substitutions in Ang1 (I434M and F469L), and two others (K432N and Y475H) are also likely to have little or no effect on the ligand-receptor interactions. Thus, there are only three Tie2-contacting residues different between Ang1 and Ang2 (N468G, S417I and S480P) that might affect the ligand-receptor interactions. One of these, Asn468, is actually involved in energetically unfavorable van der Waals contacts with Tie2 Ile162 and Phe161, and its substitution with glycine in Ang1 would facilitate stronger receptor binding. Ser417 and Ser480 of Ang2, by contrast, make hydrogen bonds with His168 and Ser164 of Tie2, respectively, and their substitutions with isoleucine and proline in Ang1 would abolish these bonds. Nevertheless, these substitutions might not be energetically very unfavorable, as the nonpolar side chains of Ile417 and Pro480 in Ang1 are likely to engage in favorable hydrophobic interactions with the nonpolar side chain atoms of Tie2 His168 and His163, respectively. In aggregate, the Ang2–Tie2 structure suggests that the Ang1–Tie2 complex is likely to have a very similar three-dimensional architecture.

To evaluate whether the above-stated structure-based predictions are valid and whether Ang1 and Ang2 indeed use the same binding site on Tie2, we altered crucial Tie2 residues and tested the ability of Ang1 and Ang2 to bind and activate the mutated receptors. Specifi-

cally, we generated two Tie2 variants, one containing substitutions P166E, R167E and H168A and the other containing F161A and S164E (see Fig. 5b). The first set of mutations resulted in an unstable protein, whereas the second set resulted in a protein with unaffected fold and stability. Apart from its distinct angiopoietin-binding properties, the latter mutant was biochemically indistinguishable from wild-type Tie2. *In vitro* binding studies (Fig. 3a) showed that the F161A and S164E substitutions, which are located at the center of the Ang2-Tie2 interface (Fig. 5b), abrogate binding not only to Ang2 but also to Ang1, suggesting that the ligands bind Tie2 in very similar manners. In addition to the biophysical binding experiments, we performed Tie2 receptor-activation assays in HEK293 cells (Fig. 3b). These assays revealed that both angiopoietins can efficiently induce phosphorylation of the kinase domain of wild-type Tie2 (left gels), but not of the mutant receptor (right gels). Together, these experiments confirm that both Ang1 and Ang2 can activate Tie2 via binding at the same site on its surface. They are consistent with previous reports suggesting that Ang1 and Ang2 could compete for Tie2 binding¹⁷. Recent studies of Tie2 activation in several natural and heterologous systems further indicate that not only Ang1, but also Ang2, can act agonistically *in vivo* in a context (target cell)-dependent manner. These studies have shown that the differential angiopoietin activities are controlled at the level of the target cell, differing, for example, in blood-vessel endothelial cells and lymphatic endothelial cells^{15,17,18,20,39}.

Potential differences in the multimerization states of Ang1 and Ang2 are also not likely to account for their different effects, as both molecules form similar mixtures of tetramers, pentamers, hexamers and higher-order oligomers in solution^{20,22}. Our cell-based Tie2 activation assays (Fig. 3b) further suggest that similarly oligomerized Ang1 and Ang2 elicit similar receptor responses. Thus, the results presented here support the third hypothesis outlined at the beginning of this section, namely that additional cell-specific surface receptors or coreceptors exist that could transduce or modulate the angiopoietin signals. Ang1, for example, binds $\alpha_5\beta_1$ integrin with a similar affinity as Tie2, suggesting that there is an alternative Ang1-specific receptor whose activation results in a variety of cellular responses, including cell adhesion and activation of MAP kinases⁴⁰.

DISCUSSION

It is generally thought that RTKs are activated by ligand-induced dimerization, where the approximation of two receptor molecules after ligand binding is sufficient for their activation and the initiation of downstream signaling²⁴. Ligand-induced dimerization may result either from direct binding of a single ligand molecule (or a preformed ligand dimer) to two different receptors (as in vascular endothelial growth factor)⁴¹ or from ligand-induced conformational changes in the receptor that result in its dimerization (as in EGF)^{42,43}. Tie2 activation, by contrast, requires interaction with ligands that exist *in vivo* only as multimers—tetramers, hexamers or higher-order multimers. In this respect, the angiopoietin-Tie2 system is similar to that of the Eph receptors and their ephrin ligands, which also form ligand-receptor clusters at the sites of cell-cell contact⁴⁴. In the case of Tie2, though, it has not been fully resolved whether simple dimer formation could suffice for receptor phosphorylation. To address this question, we evaluated the ability of strictly monomeric, dimeric or multimeric (preclustered) Ang1 and Ang2 to activate Tie2 expressed in HEK293 cells. Our results (Fig. 3b) indicate that neither monomeric nor dimeric ligand can result in efficient receptor activation and that ligand multimerization is a prerequisite for effective signaling. This observation is consistent with experiments reported in ref. 22, where a multimerization-deficient angiopoietin variant (Ang1C265S,

which forms tetramers but not higher-order aggregates in solution) could only weakly activate Tie2 in an endothelial cell system. Thus, our data supports a model for Tie2 activation illustrated in Figure 6b, where simple receptor clustering upon interaction with preclustered ligand, rather than precise orientation or positioning of receptor dimers, results in phosphorylation of the Tie2 kinase domain and initiation of downstream signaling.

METHODS

Protein expression and purification. The human Tie2 ligand-binding region (LBR) (residues 1–452) was cloned as an IgG fusion protein into a modified pcDNA3.1 vector (Invitrogen) for constitutive overexpression in a human embryonic kidney 293 (HEK293) cell line. We placed a thrombin cleavage site on the C-terminal side of the gene of interest, followed by the constant domain of IgG to facilitate purification. Large-scale protein expression was performed in roller-bottle culture with typical yields averaging 10 mg l⁻¹. Tie2-LBR was purified from conditioned media by affinity chromatography on protein A sepharose, cleaved from its Fc fusion tag by thrombin proteolysis and further purified by gel-filtration chromatography. The nine vector-derived residues GSASGLVPR remain at the C terminus of Tie2 after thrombin cleavage. N-terminal sequencing confirmed the identity of the purified product and identified Ala23 as the N-terminal amino acid residue of the secreted protein. Human Ang2 receptor-binding region (RBR) was expressed and purified as described¹⁹. Mouse Ang1-RBR (residues 279–498) was expressed and purified in a manner similar to Ang2-RBR.

Crystallization and structure determination of Tie2. The recombinant Tie2 ectodomain binds the angiopoietins with high affinity and specificity, as shown by analytical ultracentrifugation and gel-filtration chromatography¹⁹. The purified protein was concentrated to 20 mg ml⁻¹ in a buffer containing 10 mM bis-Tris propane (pH 7.0) and 200 mM NaCl. It was crystallized by hanging drop vapor diffusion at room temperature against a well solution of 2.0 M ammonium sulfate and 5% (w/v) PEG 400. Crystals routinely grew over

Table 1 Data collection and refinement statistics

	Tie2	Ang2-Tie2
Data collection		
Space group	<i>P</i> 4 ₁ 2 ₁ 2	<i>P</i> 4 ₁ 2 ₁ 2
Cell dimensions		
<i>a</i> , <i>b</i> , <i>c</i> (Å)	114.90, 114.90, 113.89	165.64, 165.64, 115.31
Resolution (Å)	2.8	3.5
<i>R</i> _{merge}	12.2 (48.9)	20.5 (40.3)
<i>I</i> / σ <i>I</i>	12.8 (2.4)	4.34 (1.8)
Completeness (%)	96.9 (84.6)	94.5 (91.0)
Redundancy	4.2	3.8
Wavelength	1.215 (W L-III edge)	1.1
Refinement		
Resolution (Å)	50.0–2.8	50.0–3.5
No. reflections (work/test)	26,227/2,832	32,080/1,615
<i>R</i> _{work} / <i>R</i> _{free}	24.0/29.3	27.4/32.0
No. atoms		
Protein	3,285	5,023
Ligand/ion	60/25	56/11
<i>B</i> -factors		
Protein	29.8	4.8
Ligand (NAG)/ion	66.8/61.9	33.3/6.5
R.m.s. deviations		
Bond lengths (Å)	0.008	0.010
Bond angles (°)	1.63	1.46

Each data set was collected from a single crystal. Data statistics treat Bijvoet mates independently. The values in parentheses are for the highest-resolution shell, which is 2.9–2.8 Å for Tie2 and 3.63–3.50 Å for Ang2-Tie2.

the course of 3–4 weeks, with a maximum size of $100 \times 100 \times 100 \mu\text{m}$. Native crystals were rapidly transferred to a cryo-buffer consisting of the mother liquor with an additional 25% (v/v) glycerol. For derivative preparation, crystals were transferred into a fresh drop of 2.0 M ammonium sulfate and 2 mM sodium 12-tungstophosphate ($\text{Na}_3\text{PW}_{12}\text{O}_{40}$) for 4–6 h before a quick soak in cryo-buffer containing heavy atom solution.

For structure determination, a single-wavelength data set was used, collected from a single $\text{Na}_3\text{PW}_{12}\text{O}_{40}$ derivative crystal at National Synchrotron Light Source (NSLS) Brookhaven beamline X29 at the tungsten K edge (Table 1). Oscillation photographs were integrated, merged and scaled using DENZO and SCALEPACK⁴⁵. Ten of the 12 heavy atom positions were determined with SnB⁴⁶ using the full resolution of the peak data set. Subsequent calculations were performed using autoSHARP⁴⁷ and the CCP4 suite³⁴. The experimental electron density map was of excellent quality (Supplementary Fig. 1 online), allowing the unambiguous tracing of the entire protein. The model was built using O⁴⁸ and refinement proceeded with molecular dynamics and energy minimization in CNS⁴⁹. Stereochemical analysis of the final refined model with PROCHECK³⁴ revealed side chain parameters better than or within the typical range of values for protein structures.

The final model includes residues 23–445, four *N*-acetylglucosamine groups and five SO_4 ions and is refined at 2.8-Å resolution to an *R*-factor of 24.0% and *R*_{free} of 29.3%. The structure contains 14 disulfide bonds: one in Ig1 (Cys44–Cys102), one in Ig3 (Cys370–Cys424) and four each in the EGF repeats. Notably, EGF1 and EGF3 have exactly the same topological arrangement of their disulfide bonds, whereas the topology of the disulfide bonds in EGF2 is somewhat different. Specifically, EGF1 (Tie2 residues 211–252) contains disulfide bonds Cys211–Cys220, Cys224–Cys233, Cys227–Cys240 and Cys242–Cys251; EGF2 (residues 254–300) contains disulfide bonds Cys255–Cys264, Cys268–Cys274, Cys280–Cys287 and Cys289–Cys298; and EGF3 (residues 302–343) contains disulfide bonds Cys302–Cys311, Cys315–Cys323, Cys317–Cys329 and Cys331–Cys340.

Crystallization and structure determination of the Ang2–Tie2 complex. Tie2 LBR and Ang2 RBR were mixed in a 1:2 molar ratio before gel-filtration chromatography. Purified complex was separated, pooled and concentrated to 20 mg ml⁻¹ in a buffer containing 10 mM bis-Tris propane (pH 7.0) and 200 mM NaCl. The complex was crystallized by hanging drop vapor diffusion at room temperature against a well solution of 2.2 M ammonium sulfate and 0.1 M MES (pH 6.0). Small needle-like crystals grew over the course of 3–4 weeks, with a maximum size of $200 \times 30 \times 20 \mu\text{m}$. For data collection, the crystals were rapidly transferred to a cryo-buffer consisting of the mother liquor with an additional 25% (v/v) glycerol and frozen in liquid nitrogen.

The structure of the Ang2–Tie2 complex was determined (with data collected from a single crystal) using the molecular-replacement methods and the program MOLREP from the CCP4 suite³⁴. Rotation and translation search using the structure of unbound Tie2 and the structure of unbound Ang2 previously determined by our group¹⁹ (PDB entry 1Z3S) resulted in an unambiguous solution. Manual model building was accomplished using O⁴⁸. Refinement of the model was carried out using CNS⁴⁹. Crystallographic details are presented in Table 1. The final model contains residues 23–445 of Tie2, including nine *N*-acetylglucosamine groups, and residues 280–495 of Ang2. It is refined at 3.5-Å resolution to an *R*-factor of 28.0% and *R*_{free} of 32.0%.

Structure-based mutagenesis and size-exclusion chromatography analysis.

Tie2 structure-based mutagenesis was performed using the QuikChange mutagenesis kit (Stratagene) following the manufacturers suggestions. Tie2 mutants were expressed and purified using the same protocols as with wild-type Tie2. The purified recombinant angiopoietins and Tie2 were mixed in a 2:1 molar ratio in a buffer containing 20 mM HEPES (pH 7.4) and 200 mM NaCl (HBS) and incubated for 1 h on ice before analysis. For gel filtration, 300 μl of the mixture ($\sim 2 \text{ mg ml}^{-1}$ total protein concentration) was injected onto a Superdex 200 column (10/30) (Pharmacia) pre-equilibrated in 20 mM HEPES (pH 7.4) and 200 mM NaCl. Fractions (1 ml) were collected and resolved on Coomassie-stained SDS-PAGE.

Cell-based Tie2 activation assay. For the Tie2 activation assays, HEK 293 cells (which lack endogenous Tie receptors) were stably transfected with full-length

Tie2 or the Tie2 ligand-binding mutant (F161A S164E) using Lipofectamine 2000 (Invitrogen) according to the manufacturer's recommendations. Upon reaching confluency, the Tie2-expressing cells were challenged with media containing added $\sim 0.1 \mu\text{M}$ purified recombinant Ang1-RBR, Ang2-RBR, Ang1-RBR–Fc or Ang2-RBR–Fc. Gel-filtration experiments confirmed that Ang1-RBR and Ang2-RBR were monomeric whereas Ang1-RBR–Fc and Ang2-RBR–Fc were dimeric in solution. For ligand clustering, an additional antibody to human IgG was added at a $\sim 25 \text{ nM}$ concentration. After 30 min of incubation with ligand, cells were briefly washed with cold PBS and scraped, and cells were then lysed in a buffer containing 20 mM HEPES (pH 7.4), 150 mM NaCl, 1% (w/v) NP-40 and 1 mM EDTA. Activated receptor was immunoprecipitated with the 4G10 (Upstate Biotechnology) antibody to phosphotyrosine and protein-A sepharose, resolved on SDS-PAGE and blotted onto PVDF. Membranes were then probed with antibody to Tie2 (R&D Biotechnology). The total Tie2 amount was estimated from total cell lysates resolved on SDS-PAGE and probed with anti-Tie2.

Accession codes. Protein Data Bank: Coordinates have been deposited with accession codes 2GY5 (Tie2) and 2GY7 (Ang2–Tie2).

Note: Supplementary information is available on the Nature Structural & Molecular Biology website.

ACKNOWLEDGMENTS

This work was supported by the US National Institutes of Health (RO1-HL077249). We thank the staffs of beamlines X29A at the NSLS and NE-CAT at the Advanced Photon Source. Operation of the NSLS synchrotron beamline is supported by the US Department of Energy (contract no. DE-AC02-98CH10886). NE-CAT synchrotron beamline operations are supported by the National Center for Research Resources at the US National Institutes of Health (award RR-15301).

COMPETING INTERESTS STATEMENT

The authors declare that they have no competing financial interests.

Published online at <http://www.nature.com/nsmb/>

Reprints and permissions information is available online at <http://npg.nature.com/reprintsandpermissions/>

- Folkman, J. & D'Amore, P.A. Blood vessel formation: What is its molecular basis? *Cell* **87**, 1153–1155 (1996).
- Yancopoulos, G.D. *et al.* Vascular-specific growth factors and blood vessel formation. *Nature* **407**, 242–248 (2000).
- Jones, N., Ilijin, K., Dumont, D.J. & Alitalo, K. TIE Receptors: New modulators of angiogenic and lymphangiogenic responses. *Nat. Rev. Mol. Cell Biol.* **2**, 257–267 (2001).
- Carmeliet, P. & Jain, R.K. Angiogenesis in cancer and other diseases. *Nature* **407**, 249–257 (2000).
- Sato, T.N. Vascular development: molecular logic for defining arteries and veins. *Curr. Opin. Hematol.* **10**, 131–135 (2003).
- Semenza, G.L. Angiogenesis in ischemic and neoplastic disorders. *Annu. Rev. Med.* **54**, 17–28 (2003).
- Zetter, B.R. Angiogenesis and tumor metastasis. *Annu. Rev. Med.* **49**, 407–424 (1998).
- Hata, K. *et al.* Expression of angiopoietin-1, angiopoietin-2, and Tie2 genes in normal ovary with corpus luteum and in ovarian cancer. *Oncology* **62**, 340–348 (2002).
- Tanaka, S. *et al.* Tie2 vascular endothelial receptor expression and function in hepatocellular carcinoma. *Hepatology* **35**, 861–867 (2002).
- Stratmann, A., Risau, W. & Plate, K.H. Cell type-specific expression of angiopoietin-1 and angiopoietin-2 suggests a role in glioblastoma angiogenesis. *Am. J. Pathol.* **153**, 1459–1466 (1998).
- Peters, K.G. *et al.* Expression of Tie2/Tek in breast tumour vasculature provides a new marker for evaluation of tumour angiogenesis. *Br. J. Cancer* **77**, 51–56 (1998).
- Lin, P. *et al.* Inhibition of tumor angiogenesis using a soluble receptor establishes a role for Tie2 in pathologic vascular growth. *J. Clin. Invest.* **100**, 2072–2078 (1997).
- Lin, P. *et al.* Antiangiogenic gene therapy targeting the endothelium specific receptor tyrosine kinase Tie2. *Proc. Natl. Acad. Sci. USA* **95**, 8829–8834 (1998).
- Ramsauer, M. & D'Amore, P.A. Getting Tie(2)d up in angiogenesis. *J. Clin. Invest.* **110**, 1615–1617 (2002).
- Valenzuela, D.M. *et al.* Angiopoietin 3 and 4: diverging gene counterparts in mice and humans. *Proc. Natl. Acad. Sci. USA* **96**, 1904–1909 (1999).
- Davis, S. *et al.* Isolation of Angiopoietin-1, a ligand for the Tie2 receptor by secretion-trap expression cloning. *Cell* **87**, 1161–1169 (1996).
- Maisonpierre, P.C. *et al.* Angiopoietin-2, a natural antagonist for Tie2 that disrupts in vivo angiogenesis. *Science* **277**, 55–60 (1997).
- Fiedler, U. *et al.* Angiopoietin-1 and Angiopoietin-2 share the same binding domains in the Tie2 receptor involving the first Ig-like loop and the epidermal growth factor-like repeats. *J. Biol. Chem.* **278**, 1721–1727 (2003).

19. Barton, W.A., Tzvetkova, D. & Nikolov, D.B. Structure of the Angiopoietin-2 receptor binding-domain and identification of surfaces involved in receptor recognition. *Structure* **13**, 825–832 (2005).
20. Davis, S. *et al.* Angiopoietins have distinct modular domains essential for receptor binding, dimerization, and superclustering. *Nat. Struct. Biol.* **10**, 38–44 (2003).
21. Ward, N.L. & Dumont, D.J. The angiopoietins and Tie2/Tek: adding to the complexity of cardiovascular development. *Semin. Cell Dev. Biol.* **13**, 19–27 (2002).
22. Kim, K.-T. *et al.* Oligomerization and multimerization are critical for Angiopoietin-1 to bind and phosphorylate Tie2. *J. Biol. Chem.* **280**, 20126–20131 (2005).
23. Wiesmann, C., Muller, Y.A. & de Vos, A.M. Ligand-binding sites in Ig-like domains of receptor tyrosine kinases. *J. Mol. Med.* **78**, 247–260 (2000).
24. Hubbard, S.R. & Till, J.H. Protein tyrosine kinase structure and function. *Annu. Rev. Biochem.* **69**, 373–379 (2000).
25. Dumont, D.J., Yamaguchi, T.P., Conlon, R.A., Rossant, J. & Breitman, M.L. *tek*, a novel tyrosine kinase gene located on mouse chromosome 4, is expressed in endothelial cells and their presumptive precursors. *Oncogene* **7**, 1471–1480 (1992).
26. Ziegler, S.F., Bird, T.A., Schneringer, J.A., Schooley, K.A. & Baum, P.R. Molecular cloning and characterization of a novel receptor protein tyrosine kinase from human placenta. *Oncogene* **8**, 663–670 (1993).
27. Harpaz, Y. & Chothia, C. Many of the immunoglobulin superfamily domains in cell adhesion molecules and surface receptors belong to a new structural set which is close to that containing variable domains. *J. Mol. Biol.* **238**, 528–539 (1994).
28. Casasnovas, J.M., Stehle, T., Liu, J.H., Wang, J.H. & Springer, T.A. A dimeric crystal structure for the N-terminal two domains of intercellular adhesion molecule-1. *Proc. Natl. Acad. Sci. USA* **95**, 4134–4139 (1998).
29. Freigang, J. *et al.* The crystal structure of the ligand binding module of axonin-1/TAG-1 suggests a zipper mechanism for neural cell adhesion. *Cell* **101**, 425–433 (2000).
30. Zdanov, A. *et al.* Structure of a single-chain antibody variable domain (Fv) fragment complexed with a carbohydrate antigen at 1.7 Å resolution. *Proc. Natl. Acad. Sci. USA* **91**, 6423 (1994).
31. Breithaupt, C. *et al.* Structural insights into the antigenicity of myelin oligodendrocyte glycoprotein. *Proc. Natl. Acad. Sci. USA* **100**, 9446 (2003).
32. Yee, V.C. *et al.* Crystal structure of a 30 kDa C-terminal fragment from the γ chain of human fibrinogen. *Structure* **5**, 125–138 (1997).
33. Pratt, K.P., Cote, H.C.F., Chung, D.W., Stenkamp, R.E. & Davie, E.W. The primary fibrin polymerization pocket: Three-dimensional structure of a 30 kDa C-terminal γ chain fragment complexed with the peptide Gly-Pro-Arg-Pro. *Proc. Natl. Acad. Sci. USA* **94**, 7176–7181 (1997).
34. Collaborative Computational Project Number 4. The CCP4 suite: programs for X-ray crystallography. *Acta Crystallogr. D Biol. Crystallogr.* **50**, 760–763 (1994).
35. Braden, B.C. & Poljak, R.J. Structural features of the reactions between antibodies and protein antigens. *FASEB J.* **9**, 9–16 (1995).
36. Sundberg, E.J. & Mariuzza, R.A. Molecular recognition in antibody-antigen complexes. *Adv. Protein Chem.* **61**, 119–160 (2002).
37. Kairies, N. *et al.* The 2.0 Å crystal structure of tachylectin 5A provides evidence for the common origin of the innate immunity and the blood coagulation systems. *Proc. Natl. Acad. Sci. USA* **98**, 13519–13524 (2001).
38. Stein, E. *et al.* Eph receptors discriminate specific ligand oligomers to determine alternative signaling complexes, attachment, and assembly responses. *Genes Dev.* **12**, 667–678 (1998).
39. Gale, N.W. *et al.* Angiopoietin-2 is required for postnatal angiogenesis and lymphatic patterning, and only the latter role is rescued by Angiopoietin-1. *Dev. Cell* **3**, 411–423 (2002).
40. Carlson, T.R., Feng, Y., Maisonpierre, P.C., Mrksich, M. & Morla, A.O. Direct cell adhesion to the angiopoietins mediated by integrins. *J. Biol. Chem.* **276**, 26516–26525 (2005).
41. Wiesmann, C. *et al.* Crystal structure at 1.7 Å resolution of VEGF in complex with domain 2 of the Fit-1 receptor. *Cell* **91**, 695–704 (1997).
42. Ogiso, H. *et al.* Crystal structure of the complex of human epidermal growth factor and receptor extracellular domains. *Cell* **110**, 775–787 (2002).
43. Garrett, T.P. *et al.* Crystal structure of a truncated epidermal growth factor receptor extracellular domain bound to transforming growth factor alpha. *Cell* **110**, 763–773 (2002).
44. Himanen, J.P. & Nikolov, D.B. Eph signaling: a structural view. *Trends Neurosci.* **26**, 46–51 (2003).
45. Otwinowski, Z. & Minor, W. Processing of X-ray diffraction data collected in oscillation mode. *Methods Enzymol.* **276**, 307–326 (1997).
46. Weeks, C.M. & Miller, R. The design and implementation of *SnB* v2.0. *J. Appl. Crystallogr.* **32**, 120–124 (1999).
47. Evans, G. & Brice, G. Triiodide derivatization and combinatorial counter-ion replacement: two methods for enhancing phasing signal using laboratory Cu K α X-ray equipment. *Acta Crystallogr. D Biol. Crystallogr.* **58**, 976–991 (2002).
48. Jones, T.A., Zou, J.Y., Cowan, S.W. & Kjeldgaard, M. Improved methods for building protein models in electron density maps and the location of errors in these models. *Acta Crystallogr. A* **47**, 110–119 (1991).
49. Brunger, A.T. *et al.* Crystallography and NMR system (CNS): A new software system for macromolecular structure determination. *Acta Crystallogr. D Biol. Crystallogr.* **54**, 905–921 (1998).